ACS Catalysis

Research Article

pubs.acs.org/acscatalysis

Exceptional Photocatalytic Activity of 001-Facet-Exposed TiO_2 Mainly Depending on Enhanced Adsorbed Oxygen by Residual Hydrogen Fluoride

Yunbo Luan,[†,‡] Liqiang Jing,[*,†] Ying Xie,[†] Xiaojun Sun,[‡] Yujie Feng,[*,‡] and Honggang Fu[*,†]

[†]Key Laboratory of Functional Inorganic Materials Chemistry (Heilongjiang University), Ministry of Education, School of Chemistry and Materials Science, Harbin 150080, P. R. China

[‡]State Key Lab of Urban Water Resource and Environment (Harbin Institute of Technology), Harbin 150001, P. R. China

Supporting Information

ABSTRACT: Is it true that the exceptional photocatalytic activity of 001-facet-exposed TiO_2 is attributed to its high-energy surfaces? In this work, nanocrystalline anatase TiO_2 with different percentages of the exposed (001) facet has been controllably synthesized with a hydrothermal process using hydrofluoric acid as a morphology-directing agent. It is shown that the percentage of (001)-facet exposure is tuned from 6 to 73% by increasing the amount of used hydrofluoric acid, and meanwhile the amount of residual fluoride in the as-prepared TiO_2 is gradually increased. As the percentage of (001) facet is increased, the corresponding TiO_2 gradually exhibits much high photocatalytic activity for degrading gas-phase acetaldehyde and liquid-phase phenol. It was unexpected that the photocatalytic activity would obviously decrease when the residual fluoride was washed off with NaOH solution. By comparing F-free 001-facet-exposed TiO_2 with the F-residual one, it is concluded that the exceptional photocatalytic activity of the as-prepared 001-facet-exposed TiO_2 depends mainly on the residual hydrogen fluoride linked to the surfaces of TiO_2 via the coordination bonds between Ti^{4+} and F^-, as well as slightly on the high-energy 001-facet exposure, by means of the temperature-programmed desorption (TPD) measurements, the atmosphere-controlled surface photovoltage spectra, and the isoelectric point change. On the basis of the O_2-TPD tests, theoretical calculations, and O_2 electrochemical reduction behaviors, it is further suggested for the first time that the residual hydrogen fluoride as the form of −Ti:F−H could greatly enhance the adsorption of O_2 so as to promote the photogenerated electrons captured by the adsorbed O_2, leading to the great increase in the charge separation and then in the photocatalytic activity. This work would clarify the high-activity mechanism of widely investigated TiO_2 with high-energy 001-facet exposure and also provide feasible routes to further improve photocatalytic activity of TiO_2 and other oxides.

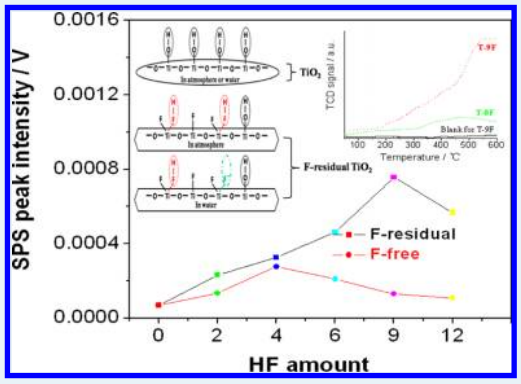

KEYWORDS: *exposed 001 facet, charge separation, residual hydrogen fluoride, adsorbed oxygen, TiO_2 photocatalysis*

1. INTRODUCTION

Titanium dioxide (TiO_2) has been intensively investigated due to its unique properties and many promising applications in environmental and energy areas.[1−3] In general, the photocatalytic performance of TiO_2 is strongly dependent on its crystal phase, crystallinity, particle size, surface area, and so on.[4−6] Widely accepted, exposed high-energy facets are favorable for efficient photocatalysis.[7,8] For anatase TiO_2, the (001) surface is more active than the (101) one on the basis of theoretical studies.[9,10] Normally, it is usually exposed with a (101) facet due to its being thermodynamically stable with a low surface energy (0.44 $J{\cdot}m^{-2}$). However, the (001) facet with a high surface energy (0.90 $J{\cdot}m^{-2}$) is difficult to expose. A pioneering breakthrough in the synthesis of anatase TiO_2 with an exposed (001) facet was achieved by Yang et al.,[11] mainly by using hydrofluoric acid (HF) as a structure-directing agent. Following the breakthrough, increasingly attention has focused on the high-energy (001) facet in order to accomplish efficient photocatalysis of anatase TiO_2.

Some researchers have demonstrated that anatase TiO_2 with a large percentage of the (001) facet exhibits high photocatalytic activity. Yang et al.[12] and Han et al.[13] synthesized anatase TiO_2 nanosheets with 64% and 89% (001) facet, respectively. The as-prepared nanosheets both exhibited much higher photocatalytic activity than P25 TiO_2. It was suggested that the high photocatalytic activity of anatase TiO_2 with a high percentage of (001) facet was ascribed to the (001)-facet exposure. However, Pan et al.[14] and Zheng[15] et al. suggested that the high percentage of (001)-facet exposure was unfavorable to improving photoactivity. After the residual fluoride, as an indispensable agent to control (001)-facet

Received: February 2, 2013
Revised: April 28, 2013

   dx.doi.org/10.1021/cs400216a | ACS Catal. 2013, 3, 1378−1385

growth, was washed off with NaOH solution, F-free anatase TiO_2 with 82% (001)-facet exposure displayed lower photoactivity than that with a 45% one.[15] Naturally, let us wonder if the high percentage of (001)-facet exposure is truly favorable for efficient photocatalysis of TiO_2.

In general, the formation of (001)-facet exposed TiO_2 mainly depends on the presence of rich fluorine under acidic conditions, which is attributed to the strong coordination actions between Ti^{4+} and F^-.[11,16] Thus, there should be some residual fluoride on the surfaces of (001)-facet exposed TiO_2. The residual fluoride, along with surface fluorination, would alter the surface properties of TiO_2, so as to influence its photocatalytic activity.[17,18] However, as for the effects of residual fluoride on the photocatalytic activity, there are still some controversies in the reported literatures so far.[19−21] In addition, for the high percentage of (001)-facet exposure and the residual fluoride, which is the determining factor for efficient photocatalysis of TiO_2? It is widely accepted that the step where the adsorbed O_2 captures photogenerated electrons is crucial for efficient photocatalytic processes.[22,23] However, it is often neglected. In our recent works,[24−26] we have demonstrated that the phosphate modification is favorable to enhancing the adsorption of O_2, leading to the increase in the charge separation and then in the photocatalytic activity of TiO_2, mainly by means of a self-built atmosphere-controlled surface photovoltage technique. To clearly reveal the roles of the high percentage of (001)-facet exposure and the residual fluoride in photocatalysis, it is indispensable to investigate their effects on the adsorbed O_2 and then on charge separation. To the best of our knowledge, related works have not been reported up to now.

Herein, we have successfully synthesized different-percentage (001)-facet exposed anatase TiO_2 using HF-modified hydrothermal processes and investigated the roles of the high-energy facet exposure and the residual fluoride in the photocatalysis of TiO_2. It is suggested for the first time that the exceptional photocatalytic activity of TiO_2 with large-percentage (001)-facet exposure for degrading colorless pollutants mainly depends on the residual hydrogen fluoride, as well as on the high-energy (001)-facet exposure, and the residual hydrogen fluoride is very favorable for the adsorption of O_2 so as to promote the photogenerated electrons captured by the adsorbed O_2, leading to high charge separation and then to high photocatalytic activity. This work would help us well understand the key factors in the photodegradation of pollutants over TiO_2 with exposed (001) facet and provide a new idea for the synthesis of high-activity oxide-based photocatalysts with high-energy facet exposure.

2. EXPERIMENTAL SECTION

All substances used in this study are of analytical grade and used without further purification. Deionized water is used in all experiments.

2.1. Synthesis of Materials. Nanosized TiO_2 with different-percentage (001)-facet exposure is controllably prepared according to a HF-modified hydrothermal method as follows.[15,27] In a typical procedure, 5 mL of $Ti(OBu)_4$ is mixed with 20 mL of absolute ethanol under vigorous stirring. Then, a certain volume (0−1.2 mL) of 40% HF solution is added. After continuously stirring for 1 h, the resulting solution is transferred to a Teflon lined stainless-steel autoclave and then kept at 160 °C for 24 h. After being cooled to room temperature, the white precipitate is collected and washed with ethanol and water several times in turn. Finally, the nanosized TiO_2 powder is obtained by drying at 80 °C for 12 h. The obtained powder is denoted as T-XF, in which T means TiO_2, F is HF, and X represents the volume of added HF in the synthesis. In addition, to remove the surface residual fluoride, the as-prepared TiO_2 powder is washed with 0.1 M NaOH solution and then distilled water several times and finally dried at 80 °C for 12 h. For comparison, HF-modified T-0F was prepared by immerging 1 g of T-0F in 100 mL of different concentrations of HF solution and then stirring for 1 h, followed by washing with deionized water and drying at 80 °C.

To carry out photoelectrochemical (PEC) measurements, as-obtained TiO_2 film electrodes are prepared.[26] The 0.3 g TiO_2 powders are dispersed in 2 mL of iso-propyl alcohol, 0.15 g of Macrogol-6000, and 0.15 mL acetylacetone in an orderly fashion under ultrasonic and vigorous stirring, and after stirring for 1 day, the resulting TiO_2 paste is obtained. Conductive fluorine-doped tin oxide (FTO)-coating glasses are cleaned by successive sonicate in acetone and deionized water for 1 h prior to use as the substrates for the TiO_2 films. The TiO_2 paste covered the FTO glasses according to the doctor blade method and then was sintered at 450 °C for 0.5 h. Finally, the TiO_2 film on FTO glass is cut into 1.7 × 3.0 cm^2 pieces with an exposed TiO_2 surface area of 1.7 × 1.5 cm^2 to use for a photoanode material. To make a photoelectrode, an electrical contact is made with the FTO substrate by using silver conducting paste connected to a copper wire which is then enclosed in a glass tube.

2.2. Characterization of Materials. The samples are tested using X-ray powder diffraction (XRD) with a Rigaku D/MAX-rA powder diffractometer, using Cu Kα radiation. Electron micrographs are taken on a JEOL JEM-2010 transmission electron microscope (TEM) operated at 200 kV. The specific surface areas of the samples are measured with a Brunauer−Emmett−Teller (BET) instrument (Micromeritics automatic surface area analyzer Gemini 2360, Shimadzu), with nitrogen adsorption at 77 K. The surface composition and elemental chemical state of the samples are examined by X-ray Photoelectron Spectroscopy (XPS) using a Kratos-AXIS ULTRA DLD apparatus with an Al(Mono) X-ray source, and the binding energies are calibrated with respect to the signal for adventitious carbon. The UV−vis diffuse reflectance spectra (DRS) of the samples are measured with a Shimadzu UV-2550 spectrometer. The surface photovoltage spectroscopy (SPS) measurements of the samples are carried out with a home-built apparatus that had been described in detail elsewhere.[28,29] The powder sample is sandwiched between two ITO glass electrodes, which are arranged in an atmosphere-controlled sealed container. The SPS signals are the potential barrier change of the testing electrode surface between that in the presence of light and that in the dark. Temperature-programmed desorption (TPD) of oxygen is conducted in a flow apparatus built by ourselves, which is described in our previous work.[25] Thirty milligrams of powder sample is pretreated at 270 °C for 0.5 h in an ultrahigh-purity He flow, and then the sample is to adsorb O_2 for 2 h at 25 °C. Finally, the amount of desorbed O_2 from 25 to 600 °C is monitored by a gas chromatograph (GC-2014, Shimadzu) with a TCD detector.

PEC experiments are performed in a glass cell with 0.5 M $NaClO_4$ solution as the electrolyte. The working electrode is the prepared TiO_2 film electrode. Platinum wire (99.9%) is used as the counter electrode, and a saturated KCl Ag/AgCl

dx.doi.org/10.1021/cs400216a | ACS Catal. 2013, 3, 1378−1385

electrode is used as the reference electrode. High-purity O_2 or oxygen-free N_2 gas is bubbled through the electrolyte before and during the experiments. Applied potentials are controlled by a commercial computer-controlled potentiostat (LK2006A made in China).

2.3. Photocatalytic Activity Evaluation. The activities of the samples are evaluated by photodegradation of the gas-phase acetaldehyde and liquid-phase phenol under a 150 W xenon lamp similar to solar light. A total of 0.1 g of TiO_2 sample is placed in a mixed gas system containing 810 ppm acetaldehyde, 20% O_2, and 80% N_2 to carry out photodegradation reactions for 1 h. The determination of acetaldehyde concentration is performed with a gas chromatograph (GC-2014, Shimadzu) equipped with a flame ionization detector. For photodegradation of phenol, 0.05 g of the TiO_2 sample is dispersed in 40 mL of 15 mg/L phenol solution, and then the irradiation lasts for 1 h. The phenol concentration is measured according to the 4-aminoantipyrine spectrophotometric method at the characteristic optical adsorption (510 nm) of phenol with a Shimadzu UV-2550 spectrophotometer after centrifugation.

3. RESULTS AND DISCUSSION

3.1. Structural Characterization and Surface Composition. It is confirmed from XRD patterns (Figure 1) that all

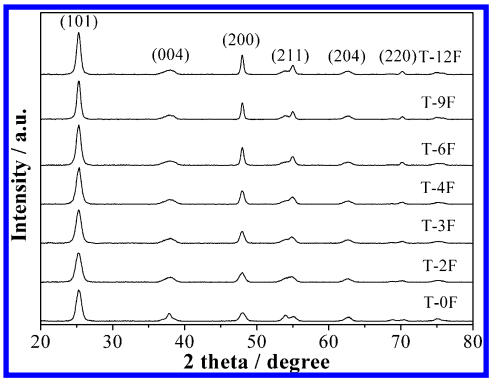

Figure 1. XRD patterns of TiO_2 samples prepared by varying the volume of HF solution from 0 to 1.2 mL.

as-prepared samples are pure anatase TiO_2. When the amount of added HF increases, the intensity of the (004) diffraction peak is decreased and its full width at half-maximum (fwhm) becomes large; meanwhile that of the (200) one is enhanced and its fwhm becomes small. This indicates that the thickness of the TiO_2 nanosheet in the [001] direction is decreased and its side length in the [100] direction becomes large with increasing the used HF amount.[30] On the basis of the thickness in the [001] direction and the side length in the [100] direction of the resulting TiO_2 nanosheet, the percentage of the exposed (001) facet is calculated,[11,30] as shown in Table 1. The percentage of the exposed (001) facet is altered from 6 to 73% as the used HF amount increases from 0 to 1.2 mL, and only 2% is increased from 0.9 to 1.2 mL. It should be pointed that the resulting TiO_2 prepared in the absence of HF is (101)-facet dominant due to its exposure of 6% of the (001) facet. In addition, the average crystallite size, evaluated using the Debye–Scherrer formula on the basis of the (101) XRD diffraction peak,[31] of the as-obtained sample is changed from 9.0 to 14.3 nm with increasing the HF amount.

Noticeably, the above dependence of exposed (001)-face percentage and the crystallite size on the added HF amount is

Table 1. XRD Data and BET Surface Areas of Different TiO_2 Samples

sample	[001] directions crystallite size (nm)	[100] directions crystallite size (nm)	exposed (001) facets (%)	average crystallite size from the (101) diffraction (nm)	tested surface area (m^2g^{-1})
T-0F	10.7	7.3	6	9.0	138
T-2F	5.7	10.6	37	9.2	112
T-3F	5.3	13.5	48	10.0	98
T-4F	5.1	17.5	57	10.7	87
T-6F	4.3	22.3	68	11.6	79
T-9F	4.0	23.1	71	12.9	73
T-12F	3.9	24.7	73	14.3	68

further confirmed by the TEM and HRTEM images (Figure 2). For in the absence of HF, the resulting TiO_2 is of octahedral

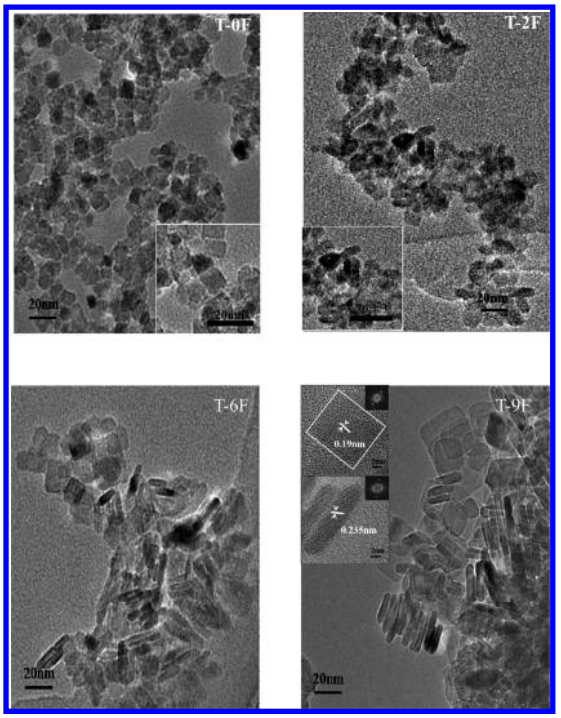

Figure 2. TEM images of T-0F, T-2F, T-6F, and T-9F TiO_2 samples.

bipyramidal shape with a width of about 8 nm and a thickness of about 10 nm. When the HF solution is introduced, nanocrystalline TiO_2 slightly grows, and its shape evolves into a truncated octahedronal bipyramid. When the volume of added HF solution rises to 0.6 mL, the truncated octahedronal bipyramid is changed to sheet-like nanostructures. If the volume of added HF solution is further increased, the side length of the TiO_2 nanosheet continues to increase, while the thickness decreases. The HRTEM images of the side view of T-9F show two sets of lattice fringes with a spacing of 0.235 and 0.19 nm, indexed to the (001) and (100) planes of the anatase phase, respectively.[27] It demonstrates that the truncated octahedral bipyramid is composed of eight equivalent (101) facets and two equivalent (001) facets. On the basis of the above structural information, the percentages of (001) facet in T-0F, T-2F, T-6F, and T-9F are estimated to be about 10, 35, 65, and 70%, respectively,[11] which is well consistent with the XRD results. One can also see from Table 1 that T-0F possesses a high surface area of 138 m^2 g^{-1}. As the percentage

dx.doi.org/10.1021/cs400216a | ACS Catal. 2013, 3, 1378–1385

of exposed (001) face increases, the surface area of the resulting TiO_2 gradually decreases. When the exposure of the (001) facet rises to 73%, the surface area of T-12F goes down as small as about 68 m^2 g^{-1}.

It is confirmed from F1s XPS spectra (Figure 3) that there is F tested on the TiO_2 prepared in the presence of HF, and the

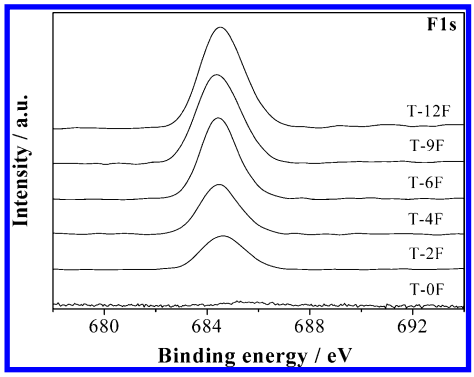

Figure 3. F1s XPS spectra of different TiO_2 samples.

XPS peak at 684.5 eV results from the surface fluoride, other than that from the fluoride doped into the crystal lattice.[32] Notably, as the used HF concentration rises, the binding energy of Ti2p slightly increases, while that of O1s is almost unchanged (Figure S1). It further confirms that the residual F is linked with Ti on the surfaces of the resulting TiO_2. In addition, it is found that the atomic concentration of F in TiO_2 gradually increases from 2.4 to 6.4% as the added HF volume is increased from 0.2 to 1.2 mL. This is in good agreement with the literature.[11,15] It has been reported that the rich fluoride is essential for preservation of the (001) facet during crystal growth, since TiO_2 termination with F atoms significantly lowers the energy of the (001) surfaces. In addition, it is naturally expected that the residual fluoride on the surfaces of (001) TiO_2 would display obvious effects on the photogenerated charge separation, similar to the surface modification with fluoride.[17,18]

3.2. Photoinduced Charge Separation. UV−vis diffuse reflectance spectra (DRS) are employed to characterize the optical properties of as-prepared samples (Figure S2). For all samples, there is obvious absorption at wavelengths lower than 400 nm, attributed to the electronic transitions from the valence band to the conduction one (O2p-Ti3d).[33,34] And, the absorption edge slightly shifts to short wavelengths with increasing HF amount. According to the respective optical absorption edge, it is evaluated that their band gap energies are about 3.2 eV.[35]

The surface photovoltage spectra (SPS) of as-obtained TiO_2 samples in the air are shown in Figure 4 for reflecting the charge separation and recombination. One can note that an obvious SPS response appears below 400 nm for all samples. This is attributed to the electronic transitions from the valence band to the conduction one (band-to-band transitions, O2p-Ti3d) on the basis of DRS spectra and TiO_2 band structure.[33,34] On the basis of the SPS responses of T-0F and T-9F in different atmospheres shown in Figure 5, it is deduced that the presence of O_2 is the necessary condition for the SPS occurrence of the resulting TiO_2,[26] and the positive photogenerated holes would preferentially diffuse to the surfaces of testing electrode since photogenerated electrons could be captured by the adsorbed O_2 according to the higher energy

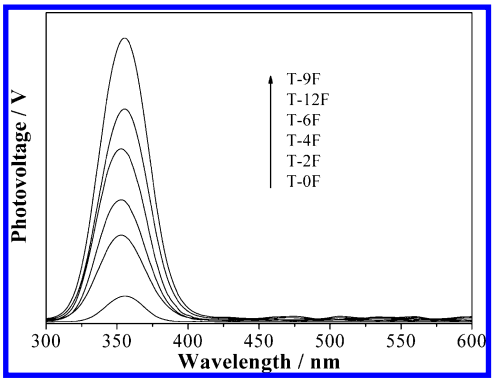

Figure 4. SPS responses of different TiO_2 samples.

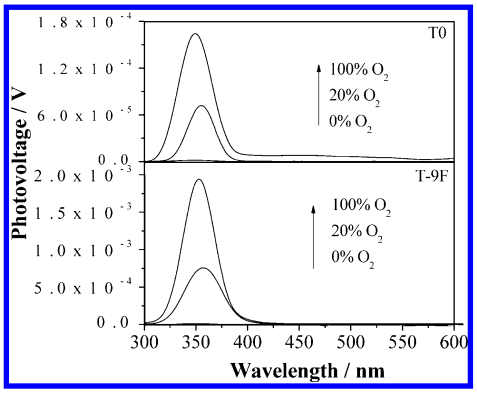

Figure 5. SPS responses of T-0F and T-9F in different O_2-concentration atmospheres.

level of the conduction bottom of the resulting TiO_2 than that of the O_2 affinity.[36,37] Noticeably, the SPS response of the resulting TiO_2 gradually becomes high with increasing the percentage of exposed (001) facet, and the T-9F with the dominant 71% (001) facet exhibits a much higher SPS response. Thus, it is concluded that the increased percentage of (001) facet is favorable to enhancing charge separation of anatase TiO_2. However, if the amount of added HF is further increased, the corresponding SPS response (T-12F with 73% (001) facet) begins to go down.

On the basis of the O_2-TPD curves shown in Figure 6 as an inset, it is confirmed that the T-9F exhibits a higher amount of O_2 desorption than the T-0F, especially for the high-temperature area. Since the adsorbed O_2 is crucial for the

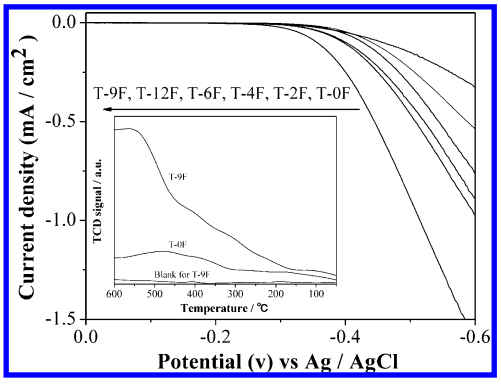

Figure 6. Electrochemical reduction of O_2 on different TiO_2 film electrodes and curves of O_2 temperature-programmed desorption of T-0F and T-9F and the blank curve of T-9F as an insert.

dx.doi.org/10.1021/cs400216a | ACS Catal. 2013, 3, 1378−1385

SPS occurrence, it is suggested that the exposure of the high-percentage (001) facet of the resulting TiO_2 is very favorable for the adsorption of O_2, leading to the strong SPS response. This is further supported by the electrochemical reduction of O_2 on the as-obtained TiO_2 film electrodes (Figure 6). Similar to the SPS response, the O_2 reduction current gradually becomes strong with increasing the percentage of (001)-facet exposure of the resulting TiO_2, and the T-9F exhibits the strongest reduction current in all samples. This demonstrates that the enhanced O_2 adsorption is responsible for its increased reduction current. However, the T-12F displays a low reduction current compared to the T-9F, which is attributed to the too large of an amount of residual fluoride unfavorable for charge transfer and separation.[25,38] According to the above results, it could be concluded that the high-percentage exposure of the high-energy (001) facet could enhance the O_2 adsorption so as to promote photogenerated electrons captured by the adsorbed O_2, leading to the charge separation improvement of the resulting TiO_2.

3.3. Photocatalytic Activity. Gas-phase acetaldehyde and liquid-phase phenol are chosen as model pollutants to evaluate photocatalytic activities of as-obtained TiO_2 under simulative solar light. The direct photolysis of the two pollutants mentioned above is neglectable compared with the photocatalytic degradation on TiO_2. The photodegradation rate is equal to the difference between the total degradation rate under illumination and the adsorption degradation rate without light, as shown in Figure 7. One can see that there is an excellent linear relationship between $\ln(C/C_0)$ (C and C_0 are concentrations of acetaldehyde or phenol after and before light irradiation, respectively) and irradiation time, indicating that the photocatalytic degradation reaction of acetaldehyde (or phenol) follows a pseudo-first-order kinetic. As expected, the photocatalytic activity of as-obtained TiO_2 is gradually enhanced with increasing the percentage of exposed (001) facet, and the T-9F with 71% (001)-facet exposure exhibits the highest activity among the resulting TiO_2. Notably, the rate constants (0.033 and 0.022 min^{-1} for photocatalytic degradation of acetaldehyde and phenol, respectively) of T-9F are larger by about 6.5 times that of the T-0F. Although T-12F possesses a higher percentage of (001)-facet exposure by 2% than T-9F, it displays a little low photocatalytic activity compared to T-9F, still much higher than T-0F. In addition, Figure S3 shows the photocatalytic degradation rates of gas-phase acetaldehyde under different O_2-content conditions, indicating that the larger is the O_2 content, the higher is the photocatalytic activity for T-0F and T-9F. Interestingly, it is found that the photocatalytic activity of as-obtained TiO_2 is in good accordance with its corresponding SPS reponses. Thus, it is deduced that the high-percentage exposure of the high-energy (001) facet corresponds to the high photogenerated charge separation, leading to the high photocatalytic activity, and the adsorbed O_2 is the determining factor for efficient photocatalysis of TiO_2.

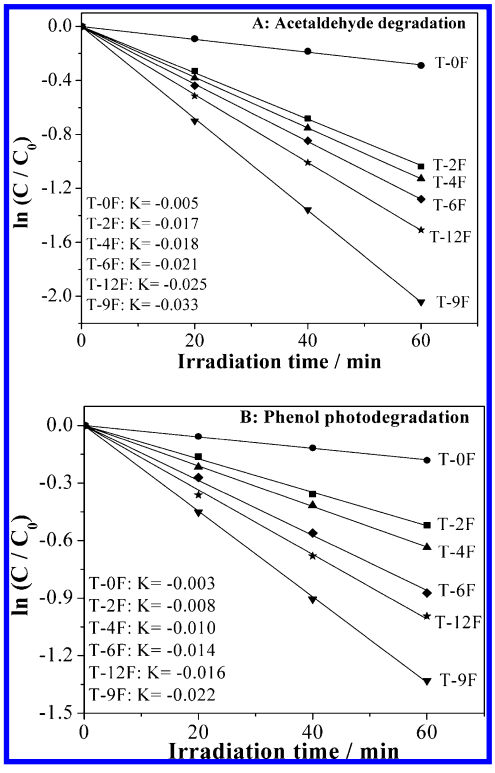

Figure 7. Photocatalytic degradation rates of gas-phase acetaldehyde (A) and liquid-phase phenol (B) on different TiO_2 samples.

3.4. Discussion. Based on the above results, it is concluded that the resulting TiO_2 with high-percentage 001-facet exposure exhibits high charge separation and high photocatalytic activity, which is attributed to the enhanced adsorption of O_2. What results from the increased O_2 adsorption? Is it true that the high-energy facet exposure is the determining factor for the adsorbed O_2? To clarify the above query, we try to remove the residual fluoride from the resulting TiO_2 by washing it with diluted NaOH solution. It could be seen from the XPS spectra in Figure S4A that the F1s XPS peak almost disappears, along with the slightly decreased binding energy of Ti2p after washing, demonstrating that the residual fluoride is removed. On the basis of the XRD patterns, DRS spectra, and SPS responses (Figure S4), it is confirmed that the percentage of (001)-facet exposure, crystallinity, energy band gap, and the SPS attribute do not change after the residual fluoride is washed off. As shown in Figure 8A, the resulting F-free TiO_2 exhibits an unexpected weak SPS response in air compared with the corresponding F-residual one. This demonstrates that the residual fluoride should play a dominant role in the photogenerated charge separation processes of TiO_2, responsible for the high photocatalytic activity. The results are consistent with some studies.[19,39] However, other studies show different results that the photocatalytic activity can be enhanced by removing F ions from the F-modified TiO_2.[13,15,40] The difference is mainly ascribed to two points. One is that a proper amount of fluoride on the surfaces of TiO_2 is important for high photoactivity, since the excessive fluoride would be unfavorable for the separation of photogenerated charges. The other is that the residual fluoride would greatly influence the adsorption of reactive substances, like O_2 and pollutants. Hence, the residual fluoride would play different roles under different conditions. In addition, it is also assured that a proper percentage of (001)-facet exposure is favorable for the increased charge separation of F-free TiO_2, and its optimal percentage of (001)-facet exposure is 57% corresponding to the added HF amount of 0.4 mL, different from that (71%) for the F-residual one. This also implies that the residual fluoride and the high-energy facet exposure have different-degree effects on the charge separation. As expected (Figure 8B), the SPS intensity of F-free TiO_2 is responsible for its corresponding photocatalytic activity for degrading gas-phase acetaldehyde and liquid-phase phenol. It

dx.doi.org/10.1021/cs400216a | ACS Catal. 2013, 3, 1378−1385

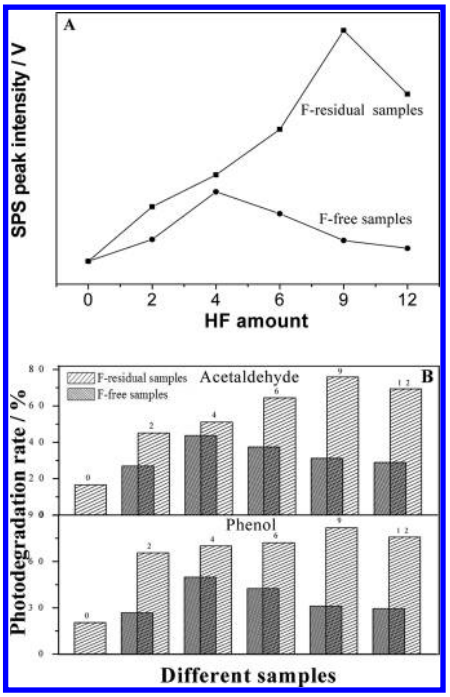

Figure 8. Intensities of SPS peak at 350 nm of resulting F-residual TiO_2 and its corresponding F-free one (A), and their photocatalytic degradation rates of gas-phase acetaldehyde and liquid-phase phenol (B).

should be pointed out that the result that a proper percentage of (001)-facet exposure of F-free TiO_2 corresponds to its high photocatalytic activity is in good agreement with the literature.[40] This is attributed to the comprehensive results from different-facet exposure, nanoparticle size, specific surface area,[15,41] and so on. In particular, the synergetic effect between the (001) and (101) facets is also important in those factors.

It is concluded that the important role of the residual fluoride is closely related to the adsorbed O_2. Why is it so favorable for the adsorption of O_2? For that, we have modified the (101)-facet dominant T-0F with different amounts of HF. One can note from Figure S5 that the HF modification does not change the phase composition from XRD patterns and energy band gap from the DRS spectra and promotes the adsorption of O_2 so as to improve photogenerated charge separation, which is responsible for the increased photocatalytic activity of T-0F modified with a proper amount of HF for degrading acetaldehyde and phenol. Obviously, the effects of modification with HF on T-0F are similar to those of the residual fluoride on the T-XF. This is explained by the same F chemical state based on their same XPS peak positions.

On the basis of the above analysis of the synthetic mechanism, along with related references,[11,16] it is naturally expected that the F^- is directly linked to Ti^{4+} on the surfaces.[11,14] If it is true, the HF-modified TiO_2 should display an isoelectric point higher than pH 7 since the strong-electronegativity F^- linked to surfaces would possibly bind a certain amount of H^+ by forming hydrogen bonds so as to make surfaces carried by positive charges. In fact, it is widely accepted that the modified TiO_2 usually possesses an isoelectric point (IEP) lower than pH 7,[17] indicating that its surfaces should be carried by negative charges. And also, it is difficult to understand why the adsorption of O_2 is promoted. Thus, in addition to the above chemical form of F^- linked to Ti^{4+}, we try to put forward a new form that the HF molecules are also linked via the nonstoichiometry coordination bonds between H−F: and Ti^{4+}. This is well supported by the following points. First, it is well-known that the coordination bonds between H−F: and Ti^{4+} are easily formed under acidic conditions.[42,43] Second, it is responsible for the IEP to change from about 6.5 (TiO_2) to about pH 3 (HF-modified TiO_2) since the HF molecule is a typical kind of weak acid with a pK_a = 3.15.[18,44] If the HF is disassociated, the surfaces would be carried by negative charges, so that its IEP should be lower than 6.5. Third, it has been suggested that the presence of the molecular form of HF but not F^- is essential for formation of the exposed (001) facets of anatase TiO_2.[45] Fourth, there are HF molecules tested in the desorbed substances by means of TPD-mass curve (Figure S6). As shown, the HF is easily desorbed at a temperature of over 525 °C. Last, what is most important is that the presence of HF is very much responsible for the markedly increased O_2 adsorption on the basis of the theoretical calculation results (SI-table 1).[46−49] One can note that the adsorption energy of O_2 with H in "−Ti:F−H" is −3.25 eV, much larger than that in "−Ti−O−H" (−0.53 eV) and that of O_2 with F in "−Ti:F" (−0.19 eV), indicating that the "−Ti:F−H" form is much more favored to adsorb O_2 compared with "−Ti−O−H" and "−Ti:F." This is also consistent with the phosphate modification (characterized by −Ti−O−P−OH or −Fe−O−P−OH) in our pervious works,[25,26] by which the attribute of surface H^+ is changed by increased acidity, favoring the O_2 adsorbed. In addition, it is expected that the "−Ti:F−H" groups lined to the surfaces would be disassociated in water, leading to the formation of a negative electric field in the surface layers of TiO_2. The formed negative field is favorable for charge separation so as to improve the photocurrent of TiO_2,[50,51] as shown in Figure S7. This is also very much responsible for the enhanced photoeletrochemical water oxidation after surface fluorination.[52]

To understand the roles of the residual fluoride, considering the above discussion, a surface structure schematic of the resulting TiO_2 prepared by HF-modified hydrothermal processes is depicted in Figure 9. As described, the surfaces

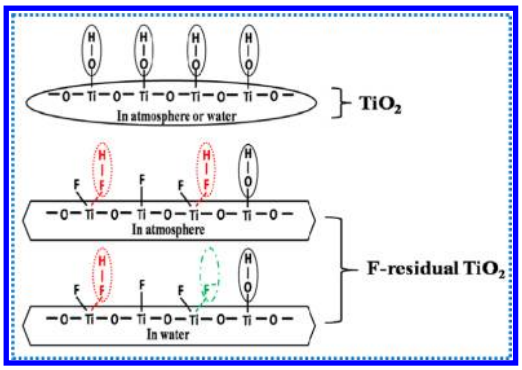

Figure 9. Surface structure schematic of common TiO_2 and the F-residual one in the atmosphere or in water.

of common TiO_2 are covered with −Ti−OH groups either in the air or in water since its IEP is near pH 7. For the resulting F-residual TiO_2, its surfaces possess −Ti−OH, −Ti−F, and −Ti:F−H groups in the air, among which the "−Ti:F−H" one is much more favored for O_2 adsorption, and in addition to −Ti−OH, −Ti−F, −Ti:F−H, its surfaces should be covered with −Ti:F^- resulting from the part disassociation of the "−

dx.doi.org/10.1021/cs400216a | ACS Catal. 2013, 3, 1378−1385

Ti:F−H" group in water. The formed negative field is beneficial for charge separation.[51] According to the surface structure scheme, we clearly demonstrate the significant effects of the residual fluoride, especially for the hydrogen fluoride, under different conditions on the photogenerated charge separation of TiO_2.

4. CONCLUSIONS

In this work, anatase TiO_2 with different percentages of exposed (001) facet is successfully obtained using the HF-modified hydrothermal process. It has been shown that, as the used HF amount increases, the percentage of (001) facet is enhanced from 6 to 73%, and simultaneously the corresponding residual fluoride increasingly remains on the surfaces of the resulting TiO_2. In the degradation of gas-phase acetaldehyde and liquid-phase phenol, the as-obtained TiO_2 displays gradually improved photoactivity with increasing the percentage of exposed (001) facet, which is mainly attributed to the enhanced adsorption of O_2, favorable to the photogenerated electrons captured by the adsorbed O_2 so as to promote the charge separation based on the O_2-TPD curves, atmosphere-controlled SPS responses, and O_2 electrochemical reduction behaviors. Moreover, by comparing the F-residual TiO_2 with the F-free one, it is further confirmed that the enhanced adsorption of O_2 is mainly related to the residual fluoride on the surfaces. Furthermore, it is suggested for the first time that the residual fluoride as the form of −Ti:F−H could greatly promote the adsorption of O_2, mainly responsible for the enhanced charge separation and then increased photocatalytic activity by means of the isoelectric point change, TPD-mass curve, and theoretical calculations. In other words, it is unexpected residual hydrogen fluoride connected to Ti-terminal surfaces via the coordination bonds that is mainly responsible for the exceptional photocatalytic activity of 001-facet-exposed TiO_2. As expected, the exposed high-energy facet is also favorable for charge separation and efficient photochemical reactions. This work would help us clearly understand the mechanism of photodegradation of pollutants over TiO_2 with exposed (001) facet and might provide feasible strategies to design and synthesize high-activity oxide-based photocatalysts with high-energy facet exposure. In addition, it should be noted that the residual hydrogen fluoride on the (001)-facet exposed anatase TiO_2 is not stable at high temperatures,[11] which would limit its application in the areas of coatings and ceramics. Attempting to solve the problem will be interesting in the future, because it seems neglected.

■ ASSOCIATED CONTENT

Supporting Information

Figure S1, XPS spectra; Figure S2, UV−vis DRS spectra; Figure S3, photocatalytic degradation rates; Figure S4, XPS spectra, XRD patterns, UV−vis DRS spectra, and SPS responses; Figure S5, XRD patterns, UV−vis DRS spectra, O_2-TPD curves, SPS responses, F1s XPS spectra, and photocatalytic degradation rates; Figure S6, desorption profiles of HF during He-TPD; SI-table 1, calculated adsorption energy for O_2 with H; Figure S7, I−V curves. This information is available free of charge via the Internet at http://pubs.acs.org/.

■ AUTHOR INFORMATION

Corresponding Author

*E-mail: Jinglq@hlju.edu.cn.

Notes

The authors declare no competing financial interest.

■ ACKNOWLEDGMENTS

We are grateful for financial support from NSFC (21071048), the Programme for Innovative Research Team in Chinese Universities (IRT1237), the Specialized Research Fund for the Doctoral Program of Higher Education (20122301110002), the Chang Jiang Scholar Candidate Programme for Heilongjiang Universities (2012CJHB003), State Key Lab of Urban Water Resource and Environment (HIT, QAK200804), and the Science Foundation of Harbin City of China (2011RFXXG001).

■ REFERENCES

(1) Chen, X. B.; Liu, L.; Yu, P. Y.; Mao, S. S. *Science* **2011**, *331*, 746−749.
(2) Chen, X. B.; Mao, S. S. *Chem. Rev.* **2007**, *107*, 2891−2959.
(3) Froschl, T.; Hormann, U.; Kubiak, P.; Kucerova, G.; Pfanzelt, M.; Weiss, C. K.; Behm, R. J.; Husing, N.; Kaiser, U.; Landfester, K.; Wohlfahrt-Mehrens, M. *Chem. Soc. Rev.* **2012**, *41*, 5313−5360.
(4) Nonoyama, T.; Kinoshita, T.; Higuchi, M.; Nagata, K.; Tanaka, M.; Sato, K.; Kato, K. *J. Am. Chem. Soc.* **2012**, *134*, 8841−8847.
(5) Tian, G. H.; Fu, H. G.; Jing, L. Q.; Xin, B. F. *J. Phys. Chem. C* **2008**, *112*, 3083−3089.
(6) Li, W.; Bai, Y.; Liu, C.; Yang, Z. H.; Feng, X.; Lu, X. H.; Laak, N. K. V. D.; Chan, K. Y. *Environ. Sci. Technol.* **2009**, *43*, 5423−5428.
(7) Liu, S. W.; Yu, J. G.; Jaroniec, M. *Chem. Mater.* **2011**, *23*, 4085−4093.
(8) Zheng, Z. K.; Huang, B. B; Qin, X. Y.; Zhang, X. Y.; Dai, Y.; Jiang, M. H.; Wang, P.; Whangbo, M. H. *Chem.−Eur. J.* **2009**, *15*, 12576−12579.
(9) Gong, X. Q.; Selloni, A. *J. Phys. Chem. B* **2005**, *109*, 19560−19562.
(10) Vittadini, A.; Selloni, A.; Rotzinger, F. P.; Grätzel, M. *Phys. Rev. Lett.* **1998**, *81*, 2954−2957.
(11) Yang, H. G.; Sun, C. H.; Qiao, S. Z.; Zou, J.; Liu, G.; Smith, S. C.; Cheng, H. M.; Lu, G. Q. *Nature* **2008**, *453*, 638−642.
(12) Yang, H. G.; Liu, G.; Qiao, S. Z.; Sun, C. H.; Jin, Y. G.; Smith, S. C.; Zou, J.; Cheng, H. M.; Lu, G. Q. *J. Am. Chem. Soc.* **2009**, *131*, 4078−4083.
(13) Han, X. G.; Kuang, Q.; Jin, M. S.; Xie, Z. X.; Zheng, L. S. *J. Am. Chem. Soc.* **2009**, *131*, 3152−3153.
(14) Pan, J.; Liu, G.; Lu, G. Q.; Cheng, H. M. *Angew. Chem., Int. Ed.* **2011**, *50*, 2133−2137.
(15) Zheng, Z. K.; Huang, B. B.; Lu, J. B.; Qin, X. Y.; Zhang, X. Y.; Dai, Y. *Chem.−Eur. J.* **2011**, *17*, 15032−15038.
(16) Zhang, D. Q.; Li, G. S.; Yang, X. F.; Yu, J. C. *Chem. Commun.* **2009**, *29*, 4381−4383.
(17) Park, H.; Choi, W. *J. Phys. Chem. B* **2004**, *108*, 4086−4093.
(18) Xu, Y. M.; Lv, K. L.; Xiong, Z. G.; Leng, W. H.; Du, W. P.; Liu, D.; Xue, X. J. *J. Phys. Chem. C* **2007**, *111*, 19024−19032.
(19) Xiang, Q. J.; Lv, K. L.; Yu, J. G. *Appl. Catal., B* **2010**, *96*, 557−564.
(20) Liu, G.; Sun, C. H.; Yang, H. G.; Smith, S. C.; Wang, L. Z.; Lu, G. Q.; Cheng, H. M. *Chem. Commun.* **2010**, *46*, 755−757.
(21) He, Z. Q.; Cai, Q. L.; Hong, F. Y.; Jiang, Z.; Chen, J. M.; Song, S. *Ind. Eng. Chem. Res.* **2012**, *51*, 5662−5668.
(22) Peiró, A. M.; Colombo, C.; Doyle, G.; Nelson, J.; Mills, A.; Durrant, J. R. *J. Phys. Chem. B* **2006**, *110*, 23255−23263.
(23) Cong, S.; Xu, Y. M. *J. Phys. Chem. C* **2011**, *115*, 21161−21168.
(24) Jing, L. Q.; Cao, Y.; Cui, H. Q.; Durrant, J. R.; Tang, J. W.; Liu, D. N.; Fu, H. G. *Chem. Commun.* **2012**, *48*, 10775−10777.
(25) Cao, Y.; Jing, L. Q.; Shi, X.; Luan, Y. B.; Durrant, J. R.; Tang, J. W.; Fu, H. G. *Phys. Chem. Chem. Phys.* **2012**, *14*, 8530−8536.
(26) Sun, W. T.; Meng, Q. Q.; Jing, L. Q.; Liu, D. N.; Cao, Y. *J. Phys. Chem. C* **2013**, *117*, 1358−1365.

(27) Yang, X. H.; Li, Z.; Sun, C. H.; Yang, H. G.; Li, C. Z. *Chem. Mater.* **2011**, *23*, 3486−3494.
(28) Jing, L. Q.; Sun, X. J.; Shang, J.; Cai, W. M.; Xu, Z. L.; Du, Y. G.; Fu, H. G. *Sol. Energy Mater. Sol. Cells* **2003**, *79*, 133−151.
(29) Luan, Y. B.; Jing, L. Q.; Meng, Q. Q.; Nan, H.; Luan, P.; Xie, M. Z.; Feng, Y. J. *J. Phys. Chem. C* **2012**, *116*, 17094−17100.
(30) Tian, F.; Zhang, Y. P.; Zhang, J.; Pan, C. X. *J. Phys. Chem. C* **2012**, *116*, 7515−7519.
(31) Kinsinger, N. M.; Wong, A.; Li, D. S.; Villalobos, F.; Kisailus, D. *Cryst. Growth Des.* **2010**, *10*, 5254−5261.
(32) Yu, J. C.; Yu, J. G.; Ho, W. K.; Jiang, Z. T.; Zhang, L. Z. *Chem. Mater.* **2002**, *14*, 3808−3816.
(33) Jing, L. Q.; Xin, B. F.; Yuan, F. L.; Xue, L. P.; Wang, B. Q.; Fu, H. G. *J. Phys. Chem. B* **2006**, *110*, 17860−17865.
(34) Kronik, L.; Shapira, Y. *Surf. Sci. Rep* **1999**, *37*, 1−206.
(35) Zhang, X.; Zhang, L. Z.; Xie, T. F.; Wang, D. J. *J. Phys. Chem. C* **2009**, *113*, 7371−7378.
(36) Thompson, T. L.; Yates, J. T. *Chem. Rev.* **2006**, *106*, 4428−4453.
(37) Wang, D. F.; Kako, T.; Ye, J. H. *J. Am. Chem. Soc.* **2008**, *130*, 2724−2725.
(38) Yu, J. G.; Wang, W. G.; Cheng, B.; Su, B. L. *J. Phys. Chem. C* **2009**, *113*, 6743−6750.
(39) Wang, Z. Y.; Lv, K. L.; Wang, G. G.; Deng, K. J.; Tang, D. G. *Appl. Catal., B* **2010**, *100*, 378−385.
(40) Zheng, Y.; Lv, K. L.; Wang, Z. Y.; Deng, K. J.; Li, M. *J. Mol. Catal. A: Chem.* **2012**, *356*, 137−143.
(41) Zhang, D. Q.; Li, G. S.; Wang, H. B.; Chan, K. M.; Yu, J. C. *Cryst. Growth Des.* **2010**, *10*, 1130−1137.
(42) Wu, G. S.; Wang, J. P.; Thomas, D. F.; Chen, A. C. *Langmuir* **2008**, *24*, 3503−3509.
(43) Zhang, H. M.; Liu, P. R.; Liu, X. L.; Zhang, S. Q.; Yao, X. D.; An, T. C.; Amal, R.; Zhao, H. J. *Langmuir* **2010**, *26*, 11226−11232.
(44) Minella, M.; Faga, M. G.; Maurino, V.; Minero, C.; Pelizzetti, E.; Coluccia, S.; Martra, G. *Langmuir* **2010**, *26*, 2521−2527.
(45) Zhang, H. M.; Wang, Y.; Liu, P.; Han, Y. H.; Yao, X. D.; Zou, J. H.; Cheng, M.; Zhao, H. J. *ACS Appl. Mater. Interfaces* **2011**, *3*, 2472−2478.
(46) Hohenberg, P.; Kohn, W. *Phys. Rev.* **1964**, *136*, B864−B871.
(47) Delley, B. *J. Chem. Phys.* **2000**, *113*, 7756−7764.
(48) Becke, A. D. *J. Chem. Phys.* **1988**, *88*, 2547−2553.
(49) Lee, C.; Yang, W. T.; Parr, R. G. *Phys. Rev. B* **1988**, *37*, 785−789.
(50) Zhao, D.; Chen, C. C.; Wang, Y. F.; Ji, H. W.; Ma, W. H.; Zang, L.; Zhao, J. C. *J. Phys. Chem. C* **2008**, *112*, 5993−6001.
(51) Jing, L. Q.; Zhou, J.; Durrant, J. R.; Tang, J. W.; Liu, D. N.; Fu, H. G. *Energ. Environ. Sci.* **2012**, *5*, 6552−6558.
(52) Monllor-Satoca, D.; Lana-Villarreal, T.; Gómez, R. *Langmuir* **2011**, *27*, 15312−15321.